Noise Behavior of Pulsed Vertical-Cavity, Surface-Emitting Lasers

T.W.S. Garrison and M. Beck

Department of Physics, Whitman College, Walla Walla, WA 99362

D.H. Christensen

National Institute of Standards and Technology, Boulder, CO 80303

Abstract

We have determined the pulse-energy fluctuations of vertical-cavity, surface-emitting lasers by measuring the number of photoelectrons produced when a laser pulse is incident on a photodetector. We obtain probability distributions for the number of photoelectrons produced by the total pulse energy, as well as distributions produced by the energy in each of the two orthogonal laser polarizations. We find that the noise of the laser increases when each new laser mode comes above threshold, and that the individual polarization outputs are noisier than the total output, indicating negative correlations between the energies in the two polarizations. We also find that while the statistics of the total output is Gaussian, this is not always true of the individual polarizations.

OCIS codes: 250.7260, 140.5960,

I. Introduction

Vertical-cavity, surface-emitting lasers (VCSELs) are microcavity lasers fabricated from semiconductor materials.[1] Because of their small size, low threshold, and high efficiency, these lasers are very interesting from both fundamental and application-minded perspectives. One area of particular interest is the investigation of the noise properties of VCSELs. From the fundamental perspective, it has been demonstrated that VCSELs can emit light with a variance that is below the shot-noise level (SNL), [2] a purely quantum mechanical effect as the SNL is the lowest noise level allowed by the semi-classical theory of photodetection.[3] From a more applied perspective, since VCSELs will play an important role in the next generation of optical communication systems, it is important to understand their noise properties.

So far nearly all studies of VCSEL noise characteristics have been performed with continuous wave (CW) lasers;[2,4-9] very little work has been done with pulsed lasers.[10,11] Measurements on pulsed lasers are important because they can provide a great deal of information on dynamical laser behavior. Also, it is pulsed lasers that will be employed in communication systems, so understanding their noise properties is of paramount importance. In the experiments that have been performed on VCSELs to date, experimenters have almost always characterized the noise either in terms of the variance of photocurrent fluctuations as a function of frequency, or in terms of the bit-error rate. No detailed measurements of probability distributions of pulsed VCSEL fluctuations have appeared in the literature.

In the experiments we have performed, we measure the number of photoelectrons produced when an optical pulse strikes a photoelectric detector. By performing an ensemble of measurements, we construct the full photoelectron distribution. We show below that for our experimental parameters the measured photoelectron number accurately reflects the pulse energy (to within our detection efficiency of 84%.)

We present measurements of photoelectron distributions for pulses emitted by VCSELs, both for the total laser output, and for the output in the two orthogonal polarizations. We find that the presence of multiple lasing modes increases the laser noise. Our measurements also show the noise levels of the individual polarizations to be greater than the noise level of the total output,[2,9] an effect similar to mode-partition noise in linearly polarized lasers.[12,13] We find that while the fluctuations of the total output are well described by Gaussian statistics, the fluctuations of the individual polarizations are not always Gaussian. Furthermore, when we compare the noise behavior of our VCSELs to that of a commercially available edge-emitting laser, we find that for pulses generating equal mean numbers of photoelectrons the VCSELs have substantially lower noise.

II. Detection System

In the semi-classical model of photoelectric detection the probability $P(n_e, t, t+T)$ of n_e photoelectrons being generated in an interval between times *t* and *t+T* can be written as [3,14]

$$P(n_e, t, t+T) = \left\langle \frac{(\gamma W)^{n_e}}{n_e!} \exp(-\gamma W) \right\rangle \ . \tag{1}$$

In this equation, γ is the efficiency of the detector in units of 1/energy; $\gamma = \eta_d / h\nu$ where η_d is the quantum efficiency of the detector, and $h\nu$ is the quantum of energy at the mean laser frequency. The integrated intensity *W* is given by

$$W = \iint_A \int_t^{t+T} I(t) dt dA \ . \tag{2}$$

In this equation the area integral is over the face of the detector. In general, the light intensity *I(t)* is a random variable, and it is being averaged over in Eq. (1). We can also regard *W* as a random variable, and express Eq. (1) in terms of it as

$$P(n_e, t, t+T) = \int_0^\infty \frac{(\gamma W)^{n_e}}{n_e!} \exp(-\gamma W) p_W(W) dW \ , \tag{3}$$

where $p_W(W)$ is the probability density of *W*. It can be shown from Eq. (3) that the mean and variance of the measured number of photoelectrons are given by

$$\langle n_e \rangle = \gamma \langle W \rangle \tag{4a}$$

$$\left\langle (\Delta n_e)^2 \right\rangle = \gamma\langle W\rangle + \gamma^2\left\langle (\Delta W)^2 \right\rangle = \langle n_e\rangle + \gamma^2\left\langle (\Delta W)^2 \right\rangle \quad . \tag{4b}$$

For our experiments, the time and space integrals in Eq. (2) are performed by the detector – the bandwidth of the detection system is such that it integrates over the entire incident pulse duration. Thus, W represents the pulse energy incident on our detector and $p_W(W)$ is the probability density of the pulse energy fluctuations. It can be seen from Eq. (4b), that there are two terms that contribute to the measured photoelectron variance – a term that is linear in the pulse energy which is called the shot-noise, and a term that is quadratic in pulse energy that is called the wave-noise.

In the limit that the wave-noise is much larger than the shot-noise, shot-noise can be ignored as a significant contributor to the measured photoelectron statistics. Furthermore, if the detector efficiency is large ($\eta_d \rightarrow 1$) and all of the pulse energy is incident the detector, the measured photoelectron statistics are an accurate representation of the pulse energy statistics. In our experiments, we estimate that our total detection efficiency is 84%, and we find that our measured photoelectron variances are always more than 15 dB above the shot-noise level. Given these two facts, the measured photoelectron statistics are an accurate reflection of the energy statistics of the light pulses.

III. Experiments

The VCSELs we have used are proton-implanted, gain-guided devices which are top-emitting at 850 nm. The current-confined implant region is 20 μm in diameter, and the emission aperture diameter is 15 μm. The gain region of the laser consists of 3 quantum wells.

A schematic of our experimental apparatus is shown in Fig. 1. In essence our experiments consisted of applying a current pulse to a VCSEL, collecting the emitted light on a photodetector, and counting the number of photoelectrons generated by the pulse. This process is repeated many times in order to measure the distribution of generated photoelectrons.

We drove the laser with 10.0 ns long voltage pulses, having rise and fall times of 2.5 ns; this produced laser pulses of 8.5 ns in duration. The pulse repetition frequency was 5 kHz. A bias tee was used to impose a 1.38 V DC bias onto these pulses. The DC bias drastically reduced ringing, producing more rectangular current pulses through the laser. We chose our bias level to be the highest voltage that would not generate any measurable CW background light from the laser; bias voltages producing laser currents of greater than about 0.1 mA were found to generate measurable background light. This CW background was found to increase the noise of our measurements, and so we kept the bias low enough to eliminate it. The current pulses through our laser were measured with a 500 MHz digital oscilloscope, which monitored the voltage across an 18Ω resistor in series with the laser.

An 11 mm focal length, 0.25 N.A., AR coated lens collected the laser light, and imaged it onto a large (1 cm^2) area detector. The detector has a quantum efficiency of 94% as specified by the manufacturer. By comparing these measurements made with the lens to others made by close-coupling the laser to the detector, we estimate that 89% of the light emitted by the laser was incident on the detector, giving us a total collection efficiency of 84%.

In our detection system the photodetector converts an optical pulse into a charge pulse. A charge-sensitive pre-amplifier and pulse-shaping amplifier convert this pulse of photoelectrons into a voltage pulse whose peak amplitude is proportional to the total charge. This peak voltage is sampled with one channel of an A/D converter and stored in the computer. Once calibrated, this measurement yields the number of generated photoelectrons for each laser pulse.[15,16] The voltage pulse emerging from the pulse-shaping amplifier is also sent into a biased amplifier, which acts as a differential amplifier to subtract a constant voltage off of the pulse, and then further amplifies the difference by another factor, adjustable between 1 and 30. This output is time delayed and then sampled by a second A/D channel. Thus, for each laser pulse we actually perform two voltage measurements. The reason for the need to make two measurements is as follows. Our A/D board has only 12-bit resolution, which is not high enough to completely resolve the fluctuations. To compensate for this, we use one channel to measure the output directly from the shaping amplifier–this measurement is used to determine the mean number of generated photoelectrons, but does not resolve the fluctuations. The biased amplifier chops off the bottom of the voltage pulse, and then further amplifies its peak–providing enough gain so that the fluctuations can be resolved.

We calibrated the detection system by illuminating the detector with a shot-noise limited train of pulses. The measured voltage V is related to the number of photoelectrons by $n_e = gV$, where g is the gain of the detection system measured in electrons/volt. A simple calculation reveals that if the detector is illuminated with a shot-noise-limited pulse train, the variance of the measured voltage fluctuations $\langle (\Delta V)^2 \rangle$ is given by [17]

$$\langle (\Delta V)^2 \rangle = \frac{\langle V \rangle}{g} + \frac{\sigma_e^{\,2}}{g^2} , \tag{5}$$

where σ_e is the standard deviation of the electronic noise (measured in electrons). By plotting the variance of V versus its mean and fitting the data, one obtains both the gain and the electronic noise of the system.

We obtained the shot-noise limited pulse train from a pulsed LED whose output was very weakly coupled into the detector. As can be seen from Eq. (4b), if the detection efficiency decreases, the wave-noise of the signal decreases more rapidly than the shot-noise (since the wave-noise is proportional to the efficiency squared). At low enough coupling efficiencies the wave-noise becomes negligible, and the shot-noise dominates.[3,18] Once this occurs, further decreases in the coupling efficiency do not change the light statistics–they remain at the shot-noise level. When calibrating with our shot-noise limited signal, we ensured that the coupling was weak enough that the measured statistics no longer depended on the coupling strength. The electronic noise σ_e of our system varied with the amplifier gain, and was found to be 580 electrons at the highest gain, and 1910 electrons at the lowest gain. For all of the measurements reported here, the measured signal variance was at least 14.7 dB above the electronic noise variance.

We varied the laser drive current from below threshold to over 2 times threshold. For each value of the applied laser drive current we detected 26,000 laser pulses and then calculated the mean and variance of this collection of pulses. We also obtained the probability distribution for the photoelectron number at a given drive current by sorting these 26,000 measurements into a histogram containing 128 bins.

IV. Discussion

In Fig. 2 we plot the mean number of detected photoelectrons $\langle n_e \rangle$ as a function of the laser current, the LI curve for our pulsed laser. Figure 2(b) contains the same data as Fig. 2(a), but is plotted on an expanded scale so that the region near threshold is more easily observed. From Fig. 2(b) it is seen that the laser threshold current is 2.9 mA. There is a kink in the LI curve at 3.5 mA, and the laser becomes more efficient above that current. Previous research has indicated that kinks in the LI curve are usually associated with additional modes coming above threshold and lasing,[4-6] and this is indeed what happens in our laser (as discussed below). Above 3.5 mA the LI curve for the total intensity is essentially linear.

It is well known that VCSELs are capable of lasing simultaneously in orthogonally polarized modes.[1] To separate these modes, we inserted a polarizer into our beam. LI curves for the two different polarizations are also shown in Fig. 2. When the laser first comes above threshold, it is linearly polarized along the direction referred to as 0^o. Below 4.2 mA of drive current the laser remains linearly polarized, and the total laser output is thus the same as the 0^o output. At 4.2 mA the laser begins to lase in the 90^o polarization as well. Close examination indicates that there is a kink in the LI curve for the 90° polarization at 5.1 mA, where the slope increases. At this same current of 5.1 mA, the slope of the LI curve for the 0° polarization decreases dramatically, as the light in the 90° polarization begins to steal more of the available gain. Eventually at 6.5 mA the 90° polarization becomes dominant. As the second polarization turns on and eventually dominates, the total laser intensity increases nearly linearly without any kinks. Thus, there is a fixed amount of gain available for the laser, and the increase in the 90° polarization comes at the expense of the 0° polarization.

We have also examined polarization resolved spectra for the laser. These spectra confirm what the LI curves seem to indicate. Just above threshold the laser lases in a single mode polarized along 0°, at a wavelength of 836.99 nm. Near 3.5 mA a second mode at λ = 836.85 nm is seen to turn on in the 0° polarization. A third mode at λ = 836.79 nm turns on at about 4.2 mA, this one lasing along the 90° polarization. A fourth mode at λ = 836.89 nm, polarized along the 90° polarization, turns on near 5.1 mA.

Figure 3 shows the variance of the photoelectron number fluctuations $\left\langle (\Delta n_e)^2 \right\rangle$ as a function of the drive current. The variance contains a series of peaks and steps. Initially, the noise is seen to increase to a peak at 2.9 mA, which corresponds to the laser threshold. Above threshold the laser noise is seen initially to decrease, as expected for a laser operating in a single mode.[19] The variance dramatically increases to a peak at 3.5 mA–precisely where the second mode turns on. The cause of this increase is evidently mode-hopping noise (a two-mode form of mode-partition noise). There is also a smaller peak in the variance at 4.3 mA, near where the third mode turns on. Another feature is evident just above 5 mA, where the fourth mode turns on. After this, the noise begins a steady increase. There is an increase in the total intensity noise of the laser in all regions where a new laser mode turns on. The most dramatic of these increases occurs where the laser goes from single-mode to multimode.

Figure 4 shows polarization resolved measurements of the photoelectron variance as a function of drive current. The most striking feature of the various variances is that the noise of the individual polarizations is greater than that of the total output. Thus, while the total intensity is relatively stable (because it is largely fixed by the total available gain), the individual polarizations are more free to fluctuate (because there is less restriction on how the gain must divide itself between the two polarizations.) Since in each laser pulse the total energy must be the sum of the energies in the two polarizations, the only way that the total noise can be quieter than the individual polarization noises is for the fluctuations in the individual polarizations to be anti-correlated. This anti-correlation between polarization modes of VCSELs has been observed before in experiments with CW lasers.[2,8]

As seen in Fig. 3, when the third and fourth modes turn on at 4.2 and 5.1 mA they have some effect on the variance of the total intensity, but the effect is relatively small. However, the turn on of the fourth mode has a very large effect on the noise of the individual polarizations, as seen in Fig. 4. In fact, the 90^{o} polarization mimics the total intensity in that when this polarization goes from single mode to multimode (at 5.2 mA), there is a dramatic increase in its photoelectron number variance.

We define the relative noise *RN* of our pulse train to be

$$RN = \frac{\left\langle (\Delta n_e)^2 \right\rangle}{\langle n_e \rangle^2} = \frac{1}{SNR^2} \quad , \tag{6}$$

where *SNR* is the signal-to-noise ratio of the pulses. This definition is in the spirit of the relative intensity noise RIN, which is a common performance measure for CW lasers. The difference is that the RIN is defined using the noise power in a certain RF spectral bandwidth, whereas there is no relevant bandwidth parameter in our measurements. Our measurements reflect the pulse-to-pulse fluctuations of the entire ensemble of measured pulses. Figure 5 shows that the general trend is for the *RN* to decrease with increasing drive current, as one expects. Features are present in the *RN* curves at the turn-on points of new modes. At the highest drive currents, the *RN* of the total intensity is over 15 dB lower than the *RN* for the individual polarizations.

A relevant question is: how much of the behavior that we observe is intrinsic to the laser, and how much might be attributed to external sources, such as noise in the pump current? We have examined the fluctuations of our pump current. At the laser threshold current of 2.9 mA the noise (the ratio of the standard deviation to the mean) of the pump current is approximately 5%, and the noise decreases as the pump current increases. At threshold, the noise on the light pulses is measured to be 6%. We therefore conclude that in the region near threshold, pump current fluctuations play a large role in determining the amount of noise on the laser pulses.

However, as described above, in Figs. 3 & 4 we see large increases in the noise precisely where new laser modes turn on. In these regions there are no corresponding increases in the pump noise, so we conclude that these increases in the noise are due to the new laser modes, not due to the pump noise. While the absolute noise level is related to the pump noise, the qualitative behavior of increasing noise when new laser modes turn on is intrinsic to the laser itself.

So far we have only discussed moments of the measured photocount statistics. However, since we measure the photoelectron number n_e in each laser pulse, we are able to determine the probability $P(n_e)\delta n_e$ that n_e will fall into a bin of width δn_e. We measure 26,000 realizations of n_e, and bin the results into normalized histograms. Each histogram has 128 equally spaced bins, in which the maximum and minimum values for n_e are the same as those in the measured data–we throw out no data points. With this convention wider distributions have larger values of the bin width δn_e. In Figs. 6 & 7 we plot the probability density of photoelectrons $P(n_e)$ as a function of n_e. The data in Fig. 6 are taken with the laser operating at a drive current of 5.0 mA, while that in Fig. 7 is for a current of 7.0 mA. In order to better compare the probability densities, all the graphs in Fig. 6 are plotted with the same scale for both vertical and horizontal axes; the same is true for Fig. 7.

In Fig. 6 the probability distribution of the total number of photoelectron counts is symmetric, while the distributions for the individual polarizations are not. The distribution of total photoelectron number shown in Fig. 6(a) is well described by a Gaussian. In Figs. 6(b) & (c), the distribution with the larger mean (0^o polarization) has a tail extending toward lower numbers of photoelectrons, while that with the smaller mean has a tail extending toward larger photoelectron numbers. The anti-correlation between the energy in the two polarizations is evident in that each of these distributions is wider than the distribution for the total energy, and by the fact that the distributions for the two polarizations are nearly mirror images of each other. The qualitative features evident in the distributions of Fig. 6, symmetric total and asymmetric individual polarizations, are found in the distributions for all drive currents between 3.0-5.2 mA.

The fact that the individual polarizations have more noise than the total intensity is strikingly evident in Fig. 7–the distributions for the individual polarizations are much broader, again evidence for anti-correlation between the fluctuations in the two polarizations. The distributions of Fig. 7 contrast with those of Fig. 6 in that all three of the measured distributions are well described by Gaussian shapes. Indeed, all the measured distributions for drive currents above 5.2 mA are essentially Gaussian. Thus, in the region where between 1 and 3 modes are lasing, the photoelectron distributions for the individual polarizations are asymmetric, while they are symmetric when four modes are lasing.

One possible explanation for the observed asymmetry in the distributions for the individual polarizations near threshold is that it may be a transient phenomena. Individual polarizations approach steady state at a rate that is proportional to the difference between the gain and the loss for that particular polarization. Thus, while the total intensity may be constant, it is possible for the intensity of the individual laser modes to still be evolving a time scale longer than the 8.5 ns duration of our pulses. Indeed, it has been observed that the time scale for the evolution of individual polarizations in a VCSEL is longer that that of the total intensity.[10] In order to test this transient hypothesis, we will need to measure the photoelectron distributions for several different pulse durations (particularly durations longer than the 8.5 ns used in these experiments).

The asymmetry may not be due to transients, however. Distributions of the intensity of individual polarizations in a CW VCSEL have been observed to be asymmetric.[9] In this case the asymmetry is presumably due to nonlinear competition between the laser polarizations. Physical models to describe this competition have been proposed,[20-23] but more work is needed to clarify the exact nature of this behavior.

Liu and coworkers have measured the distributions of individual laser modes in an edge-emitting laser (EEL), and observed behavior that is similar to what we observe in Fig. 6.[12] They found that the distribution of the total intensity is Gaussian, while the distribution for individual modes was not. Their measured distributions had tails that were similar to ours, but with one important difference. In the EEL, the distribution for the lower power mode was nearly that of an exponential peaked at zero intensity, while our distribution for the lower power mode is not peaked at zero and looks more like a Gaussian with a tail.

Direct comparisons between our experiments and those of Liu and coworkers is not really possible, because while there are some similarities between the experiments, there are numerous differences in experimental parameters. Most importantly, our measurements were performed on pulsed lasers, while Liu and coworkers repetitively sampled a CW laser. Also, one would not expect any of our measured distributions to have a peak at zero intensity; this is because in our measurements we integrate over the entire 8.5 ns duration of the pulse, a time that is much longer than the fundamental relaxation processes in the laser. Furthermore, the measurements of Ref. [12] were performed by spectrally resolving individual laser modes, which we do not do. Each polarization of our laser contains at least two transverse modes and probably several other below threshold modes.

In order to more directly compare the behavior of our VCSEL with a more traditional EEL, we have also measured the statistics of the total photoelectron number in pulses from a commercially available laser (Hitachi HL8325G) which operates in nominally the same wavelength region. The experimental procedures used for measuring the EEL were identical to those used with the VCSEL, except that the EEL was placed in series with a 40Ω resistor instead of an 18Ω resistor. Since the EEL has a much higher threshold current (35 mA) than the VCSEL, comparisons between the lasers at a given drive current are not applicable. Thus, we have chosen to compare the noises of the two lasers as a function of the mean number of detected photoelectrons per pulse. As seen in Fig. 8, the variance of the photoelectron number for the EEL is considerably larger than that of the VCSEL. We are, however, limited in the total number of photoelectrons that we can detect without saturating our detection system. Since the EEL had such a high threshold, it reached this limit at a much smaller fraction above its threshold than the VCSEL. For instance, at a mean photoelectron number of 1.5×10^7, the VCSEL was approximately 2.5 times above threshold, while the EEL was only about 9% above threshold.

V. Conclusions

We have measured the photoelectron statistics of a pulsed VCSEL. We find that the presence of multiple lasing modes significantly increases the noise in the total photoelectron number in the laser pulses. This arises from the fluctuations of individual modes in the laser as they compete for gain (mode-partition noise). The most dramatic increase in the noise is seen to occur where the laser initially goes from single-mode to multimode. We also find that the noise of the individual laser polarizations is larger than the noise in the total output, which indicates that the polarization fluctuations are anti-correlated.

Our measured photoelectron distributions indicate that the fluctuations of the total VCSEL output are Gaussian in nature. These distributions also indicate that the fluctuations of the individual polarizations are not Gaussian close to threshold (when 3 or fewer modes are lasing), but are Gaussian when 4 modes are lasing. Further experimental and theoretical investigations are necessary to fully understand this behavior.

Acknowledgments

We wish to thank M.R. Beverslius and D.S. Moore for their work on the detection system, and B.A.P. Bryan for assistance in taking the spectra. We also thank an anonymous referee for helpful suggestions. M. Beck is a Cottrell Scholar of the Research Corporation. Further support for this work came from National Science Foundation Grant No. PHY-9732453 and Whitman College.

References

[1] For a review see: C. J. Chang-Hasnain, "Vertical-Cavity Surface Emitting Lasers," in *Semiconductor Lasers Past, Present and Future*, G.P. Agrawal, ed. (AIP Press, Woodbury, NY, 1995), pp. 145-180.

[2] D.C. Kilper, P.A. Roos, J.L. Carlsten, and K.L. Lear, "Squeezed light generated by a microcavity laser," Phys. Rev. A **55**, R3323-R3326 (1997).

[3] L. Mandel and E. Wolf, *Optical Coherence and Quantum Optics*, (Cambridge Univ. Press, 1995) Ch. 9.

[4] F. Koyama, K. Morit, and K. Iga, "Intensity noise and polarization stability of GaAlAs-GaAs surface emitting lasers," IEEE J. Quantum Electron. **27**, 1410-1416 (1991).

[5] D.M. Kuchta, J. Gamelin, J.D. Walker, J. Lin, K.Y. Lau, J.S. Smith, M. Hong, and J.P. Mannaerts, "Relative intensity noise of vertical cavity surface emitting lasers," Appl. Phys. Lett. **62**, 1194-1196 (1993).

[6] L. Raddatz, I.H. White, K.H. Hahn, M.R. Tan, and S.Y. Wang, "Noise performance of multimode vertical cavity surface emitting lasers," Electron. Lett. **30**, 1991-1992 (1994).

[7] T. Mukaihara, N. Ohnoki, Y. Hayashi, N. Hatori, F. Koyama, and K. Iga, "Excess intensity noise originated from polarization fluctuation in vertical-cavity surface-emitting lasers," IEEE Photon. Technol. Lett. **7**, 1113-1115 (1995).

[8] E. Goobar, J.W. Scott, B. Thibeault, G. Robinson, Y. Akulova, and L.A. Coldren, "Calibrated intensity noise measurements in microcavity laser diodes," Appl. Phys. Lett. **67**, 3697-3699 (1995).

[9] G. Giacomelli, F. Martin, M. Gabrysch, K.H. Gulden, and M. Moser, "Polarization competition and noise properties of VCSELs", Opt. Comm. **146**, 136-140 (1998).

[10] D.V. Kuksenkov, H. Temkin, and S. Swirhun, “Polarization instability and relative intensity noise in vertical-cavity surface-emitting lasers,” Appl. Phys. Lett. **67**, 2141-2143 (1995).

[11] D.V. Kuksenkov, H. Temkin, and S. Swirhun, “Polarization instability and performance of free-space optical links based on vertical-cavity surface-emitting lasers,” IEEE Photon. Technol. Lett. **8**, 703-705 (1996).

[12] P.L. Liu, “Photon statistics and mode partition noise of semiconductor lasers,” in *Coherence, Amplification, and Quantum Effects in Semiconductor Lasers*, Y. Yamamoto ed., (Wiley, New York, 1991), pp. 411-460.

[13] J.Y. Law and G.P. Agrawal, “Mode-partition noise in vertical-cavity surface-emitting lasers,” IEEE Photon. Technol. Lett. **9**, 437-439 (1997).

[14] J.W. Goodman, *Statistical Optics*, (Wiley, New York, 1985) Ch. 9.

[15] D.T. Smithey, M. Beck, M. Belsley, and M.G. Raymer, “Sub-shot-noise correlation of total photon number using macroscopic twin pulses of light,” Phys. Rev. Lett. **69**, 2650-2653 (1992).

[16] M.E. Anderson, M. Beck, M.G. Raymer and J.D. Bierlein, “Quadrature squeezing with ultrashort pulses in nonlinear-optical waveguides,” Opt. Lett. **20**, 620-622 (1995).

[17] M. Munroe, "Ultrafast photon statistics of cavityless laser light," Ph.D. Thesis, University of Oregon, Eugene, OR, 1996.

[18] A.C. Funk and M. Beck, “Sub-Poissonian photocurrent statistics: Theory and undergraduate experiment,” Am. J. Phys. **65**, 492-500 (1997).

[19] K. Petermann, *Laser Diode Modulation and Noise* (Kluwer Academic Publishers, Dordrecht, The Netherlands, 1988) Ch. 7.

[20] K.D. Choquette, R.P. Schneider, and K.L. Lear, “Gain-dependent polarization properties of vertical cavity lasers”, IEEE J. Select. Topics Quantum Electron. **1**, 661-666 (1995).

[21] J. Martin-Regalado, S. Balle, and M. San Miguel, “Polarization and transverse-mode dynamics of gain-guided vertical-cavity surface-emitting lasers”, Opt. Lett. **22**, 460-462 (1997).

[22] A. Valle, L. Pesquera, and K.A. Shore, “Polarization behavior of birefringent multitransverse mode vertical-cavity surface-emitting lasers,” IEEE Photon. Tech. Lett. **9**, 557-559 (1997).

[23] K. Panajotov, B. Kyvkin, J. Danckaert, M. Peeters, H. Thienpont, and I. Veretennicoff, “Polarization switching in VCSEL’s due to thermal lensing,” IEEE Photon. Tech. Lett. **10**, 6-8 (1998).

Figure Captions

Fig. 1 The experimental apparatus. The polarizer was removed for measurements on the total laser output, and inserted for polarization resolved measurements.

Fig. 2 The mean number of photoelectrons $\langle n_e \rangle$ is plotted versus the laser drive current. Both total output and polarization resolved measurements are shown. (a) shows the entire range of the measurements, while (b) is plotted on an expanded scale.

Fig. 3 The variance of the measured photoelectrons $\left\langle (\Delta n_e)^2 \right\rangle$ for the total laser output is plotted versus the laser drive current.

Fig. 4 The variance of the measured photoelectrons $\left\langle (\Delta n_e)^2 \right\rangle$ is plotted versus the laser drive current. Both total output and polarization resolved measurements are shown.

Fig. 5 The relative noise *RN* [Eq. (6)] is plotted versus the laser drive current. Both total output and polarization resolved measurements are shown.

Fig. 6 Probability densities of the photoelectron number $P(n_e)$ are plotted versus n_e for (a) the total output, (b) output in the 0^o polarization and (c) output in the 90^o polarization. The laser drive current is 5.0 mA. All three plots have the same scale for vertical and horizontal axes.

Fig. 7 Probability densities of the photoelectron number $P(n_e)$ are plotted versus n_e for (a) the total output, (b) output in the 0^o polarization and (c) output in the 90^o polarization. The laser drive current is 7.0 mA. All three plots have the same scale for vertical and horizontal axes.

Fig. 8 The variance of the measured photoelectrons $\left\langle (\Delta n_e)^2 \right\rangle$ is plotted versus the mean number of photoelectrons $\langle n_e \rangle$ for both a VCSEL and an EEL.

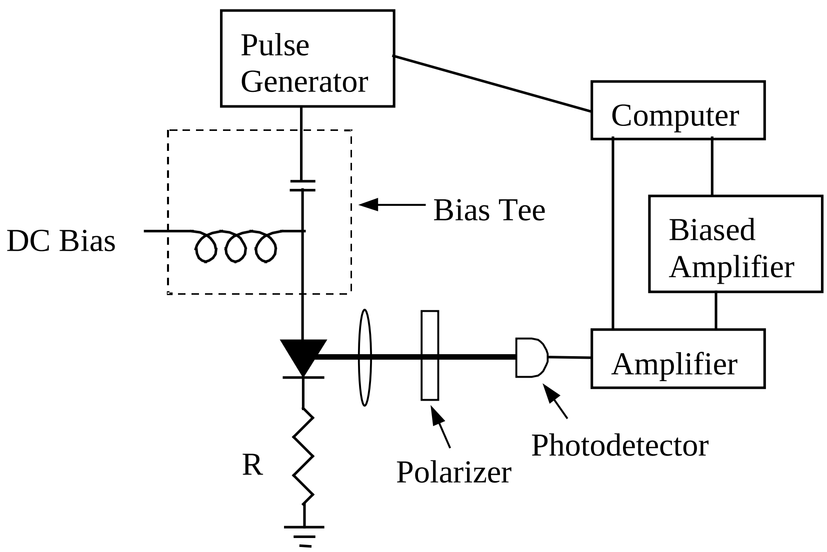
Pulse
Generator
Computer
Bias Tee
DC Bias
Biased
Amplifier
Amplifier
Photodetector
R
Polarizer

Fig. 1

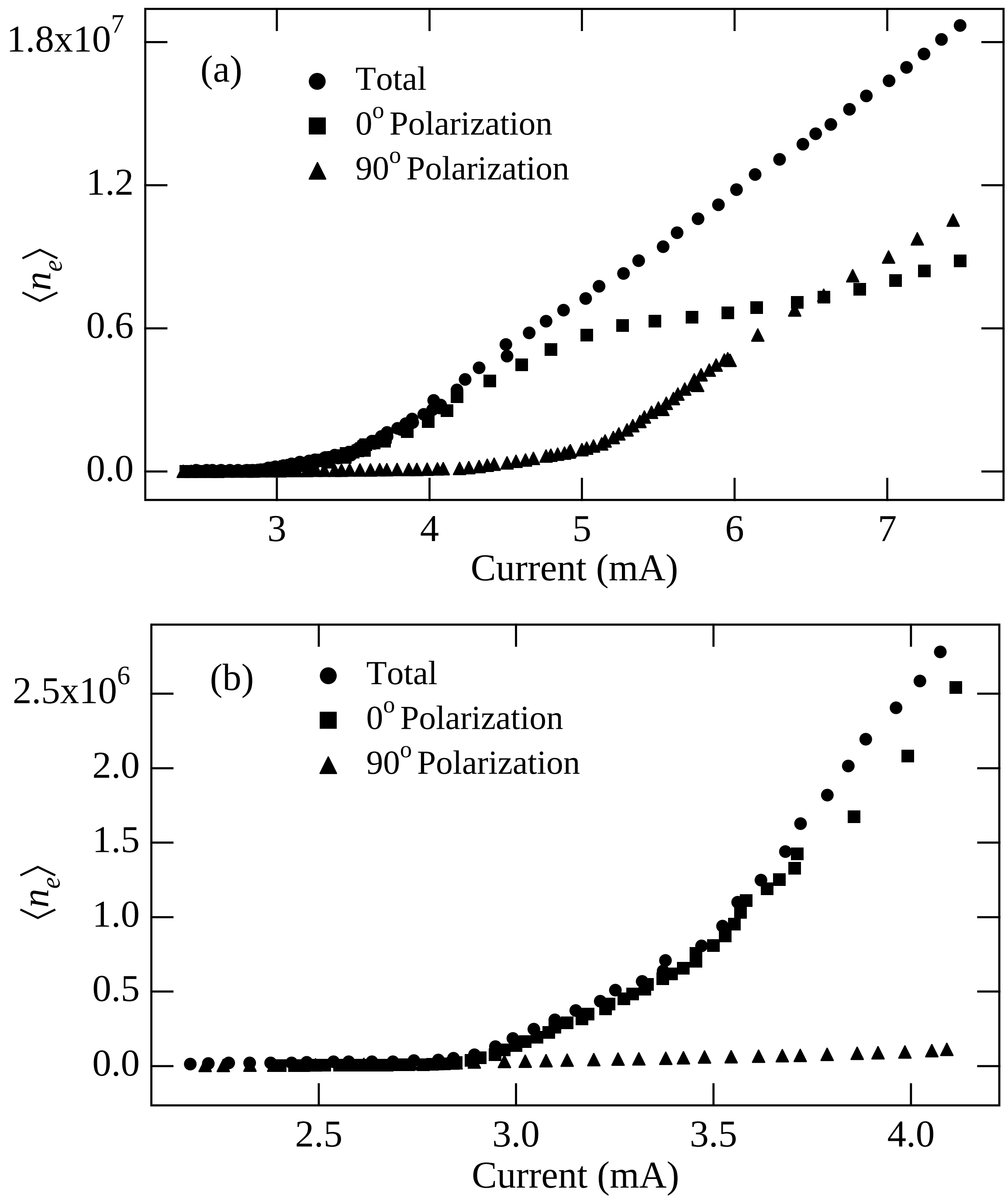
(a)
Total
0° Polarization
90° Polarization
1.8x10^7
1.2
0.6
0.0
⟨n_e⟩
3
4
5
6
7
Current (mA)
(b)
Total
0° Polarization
90° Polarization
2.5x10^6
2.0
1.5
1.0
0.5
0.0
⟨n_e⟩
2.5
3.0
3.5
4.0
Current (mA)

Fig. 2

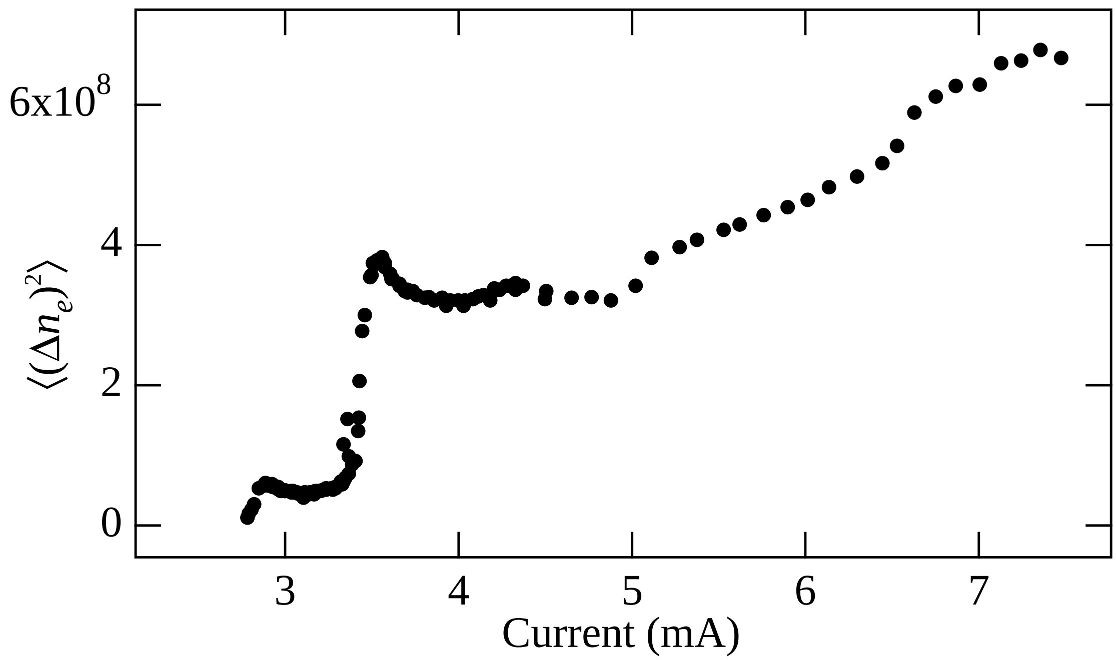

Fig. 3

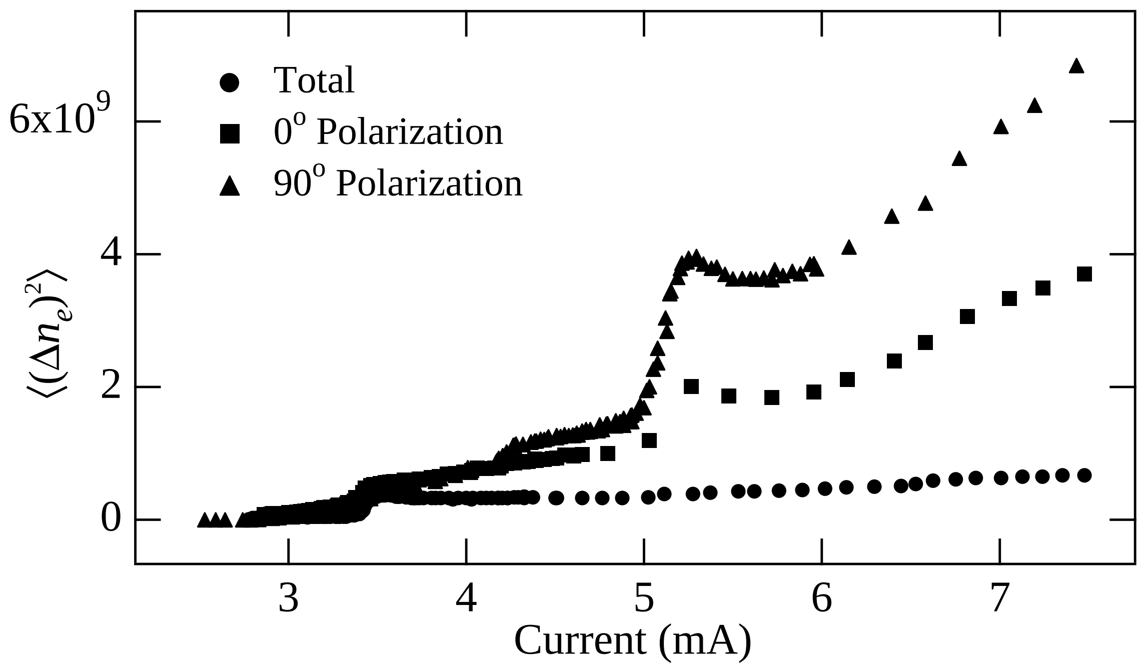
Total
0° Polarization
90° Polarization
6x10^9
4
2
0
⟨(Δn_e)^2⟩
3
4
5
6
7
Current (mA)

Fig. 4

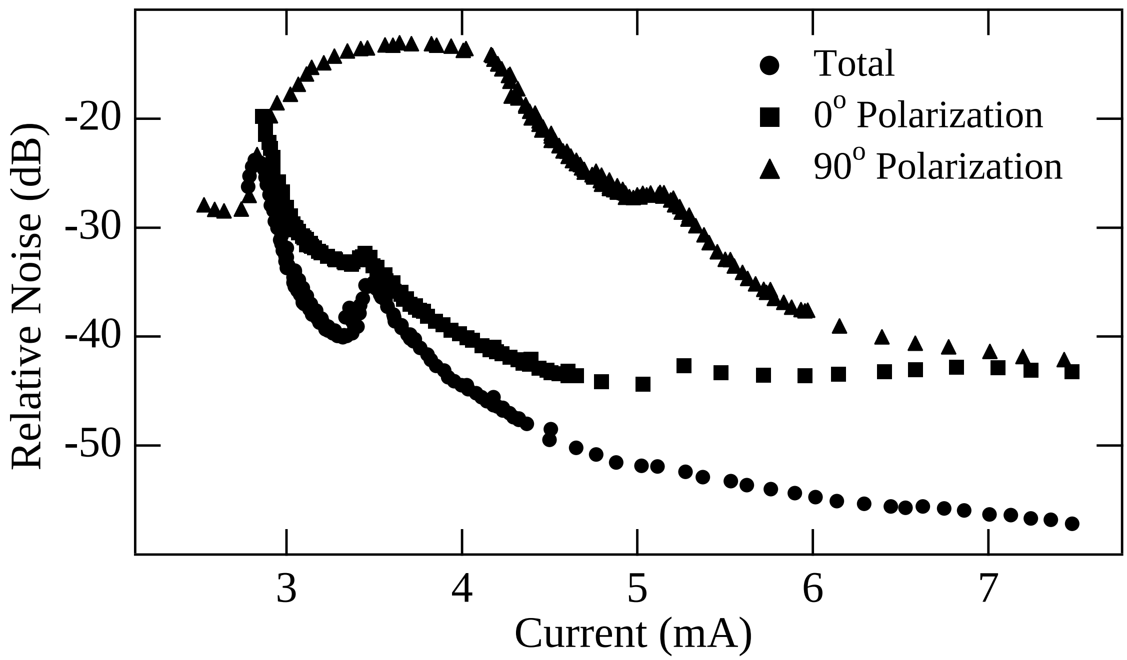
Total
0° Polarization
90° Polarization
-20
-30
-40
-50
Relative Noise (dB)
3
4
5
6
7
Current (mA)

Fig. 5

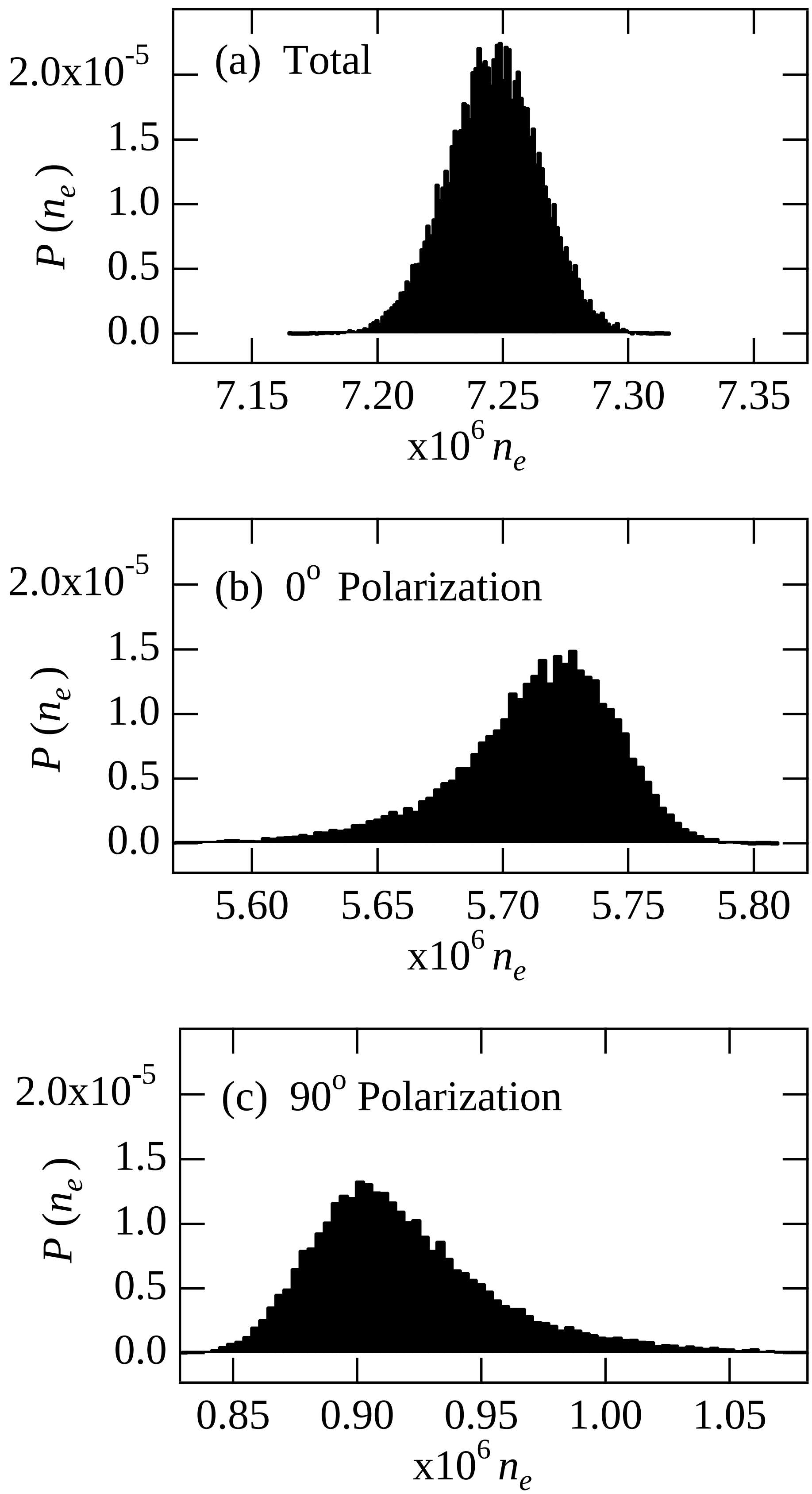
(a) Total
2.0x10-5
1.5
1.0
0.5
0.0
P (n_e)
7.15
7.20
7.25
7.30
7.35
x10^6 n_e
(b) 0° Polarization
2.0x10-5
1.5
1.0
0.5
0.0
P (n_e)
5.60
5.65
5.70
5.75
5.80
x10^6 n_e
(c) 90° Polarization
2.0x10-5
1.5
1.0
0.5
0.0
P (n_e)
0.85
0.90
0.95
1.00
1.05
x10^6 n_e

Fig. 6

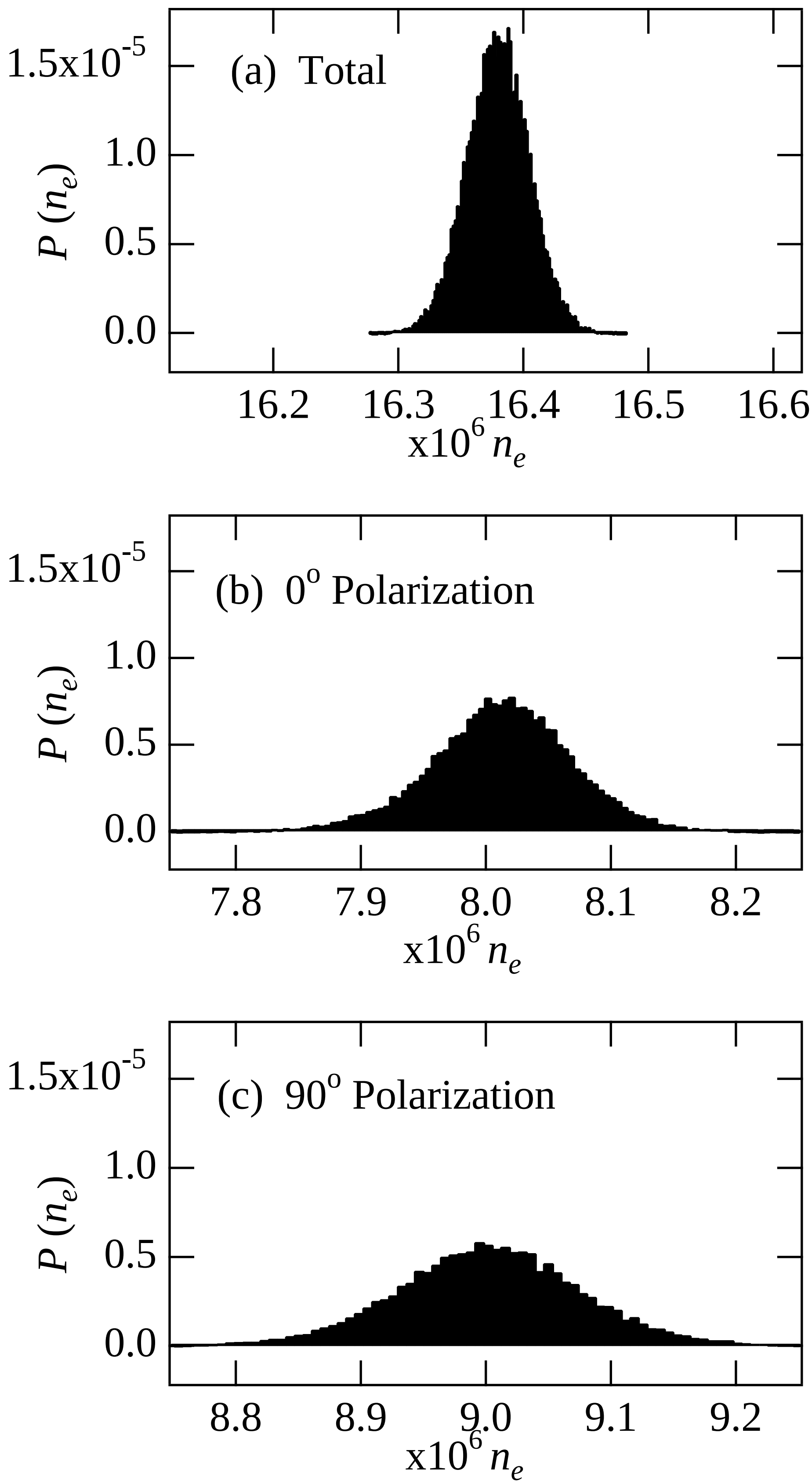

(a) Total
1.5x10^-5
1.0
0.5
0.0
P (n_e)
16.2
16.3
16.4
16.5
16.6
x10^6 n_e
(b) 0° Polarization
1.5x10^-5
1.0
0.5
0.0
P (n_e)
7.8
7.9
8.0
8.1
8.2
x10^6 n_e
(c) 90° Polarization
1.5x10^-5
1.0
0.5
0.0
P (n_e)
8.8
8.9
9.0
9.1
9.2
x10^6 n_e

Fig. 7

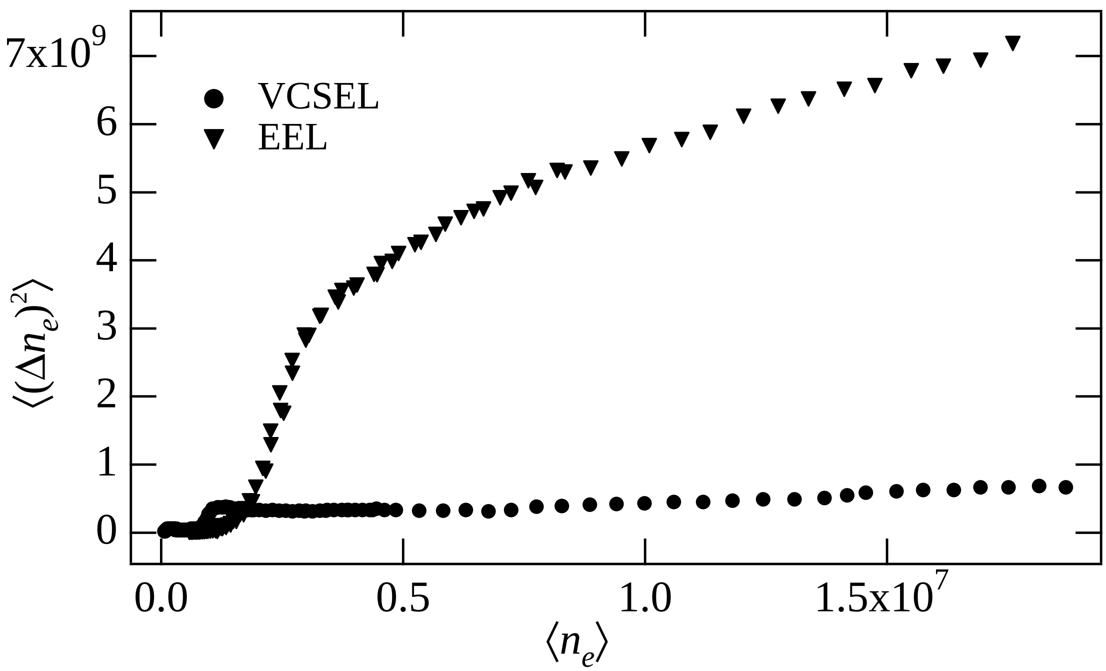

Fig. 8